

Plasma Production of Nanomaterials for Energy Storage: Continuous Gas- Phase Synthesis of Metal Oxide CNT Materials via a Microwave Plasma

Supporting Information

Brian Graves^a, Simon Engelke^{b,c}, Herme G. Baldovi^d, Jean de la Verpilliere^a, Michael
De Volder^b, Adam Boies^{a*}

^a*Department of Engineering, University of Cambridge
Trumpington Street, Cambridge, CB2 1PZ, United Kingdom*

^b*Institute for Manufacturing, University of Cambridge
17 Charles Babbage Road, Cambridge, CB3 0FS, United Kingdom*

^c*Cambridge Graphene Centre, University of Cambridge
9 JJ Thomson Avenue, Cambridge, CB3 0FA, United Kingdom*

^d*Department of Chemical Engineering and Biotechnology, University of Cambridge
Philippa Fawcett Drive, Cambridge, CB3 0AS, United Kingdom*

Additional microscopy images of the metal oxide – CNT material are shown in Figure S1. The TEM image in (a) displays a portion of an aggregate as well as catalyst primary particles trapped within CNTs and separated from the host aggregate. Figure S1 (b) and (c) show SEM and TEM images respectively of aggregate particles after CNT growth. The histogram in (d) displays the size distribution of primary particles which are responsible for CNT growth. Note that the likelihood of a particle producing CNTs decreases beyond 3 nm whereas most primary particles produced are larger than this, as seen in Figure 3f in the main article. The larger primary particles are instead often coated with graphitic carbon. Finally, Figure S1e displays the diameter distribution of the CNTs. It is right skewed with a mode at 7 nm, resulting in an average CNT diameter of 7.75 ± 2.74 nm.

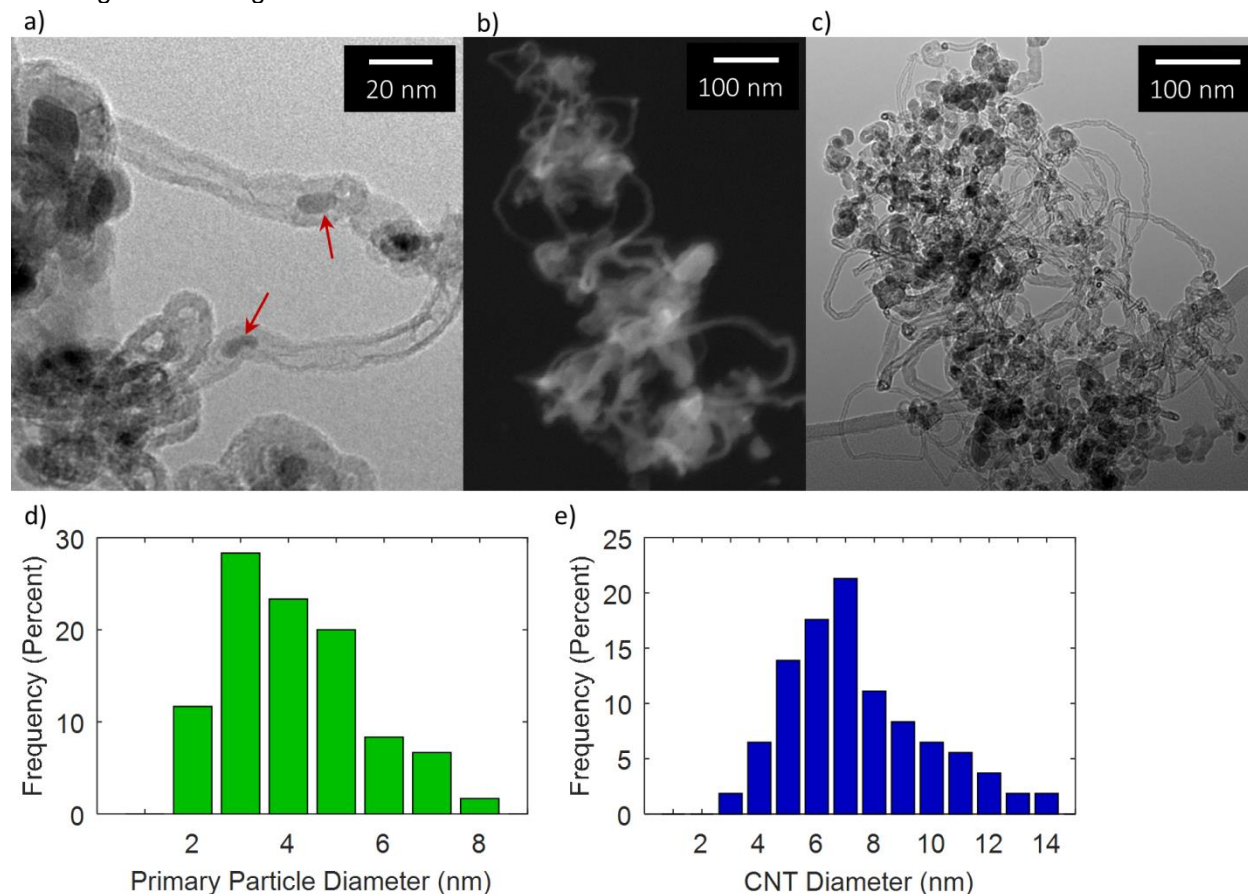


Figure S1: Additional images of material morphology including (a) TEM of a subsection of an aggregate along with primary particles contained within CNTs, (b) SEM of aggregate, and (c) TEM of large aggregate. Panel (d) displays the primary particle size distribution of those responsible for CNT growth and (e) contains the distribution of CNT diameters

A comprehensive setup is displayed in Figure S2. The process-critical elements are shown in red and include the introduction of iron and aluminum powder into the plasma along with nitrogen gas, the addition of hydrogen and acetylene post plasma, and the growth furnace. Also shown is the plasma system itself, comprised of the power supply, microwave generator (magnetron), waveguide, and microwave conditioning elements such as the 3-stub tuner and sliding short circuit. Powdered precursors are introduced with a gravity-fed rotary powder feeder and the final material is collected via filtration before the gas is vented to extraction.

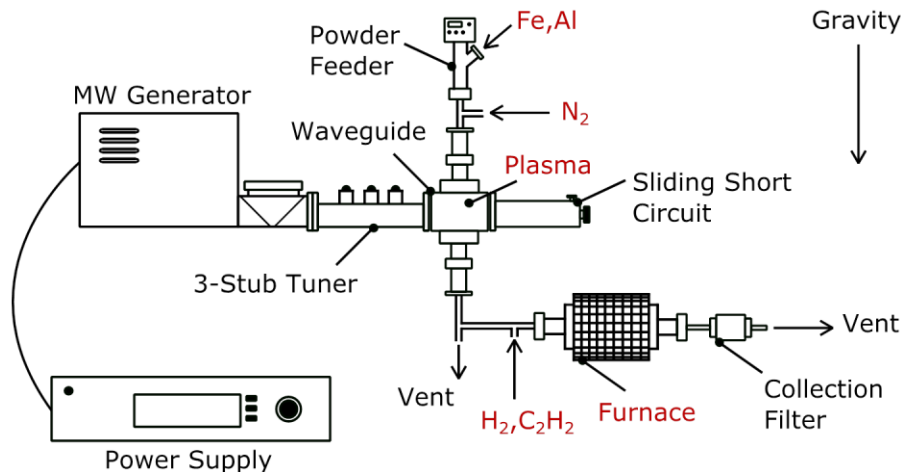


Figure S2: Comprehensive setup for material production and collection. Central process features are in red text

CV cycling was performed after the cell had been subjected to two cycles at 0.1 C. The CV data in Figure S3a is in agreement with what has been reported for iron-oxide nanoparticles elsewhere.(1) A reduction peak around 0.75 V in the cathodic sweep (corresponding to Li insertion into Fe_2O_3 and Li_2O formation) can be observed as well as an oxidation peak around 2 V in the anodic sweep (Fe^{3+} to Fe^0). Also shown is the long-term cycling in Figure S3b. The capacity is relatively steady but does increase somewhat over time. This may be due to inactive material becoming exposed from the repeated volume change during the cycling. This is a nearly unavoidable phenomenon during the initial cycles of a cell. Coulombic efficiency remains near 100% for the entirety of the long term test. Many of the individual data points throughout this test were slightly higher than 100% (though almost always less than 101%). This is likely simply due to measurement uncertainty. The several initial efficiencies near the beginning that are notably higher than 100% are the result of slightly higher discharge capacities and may be caused by irreversible reactions within the cell. These reactions are exhausted within a couple cycles at which point the cell behaves normally.

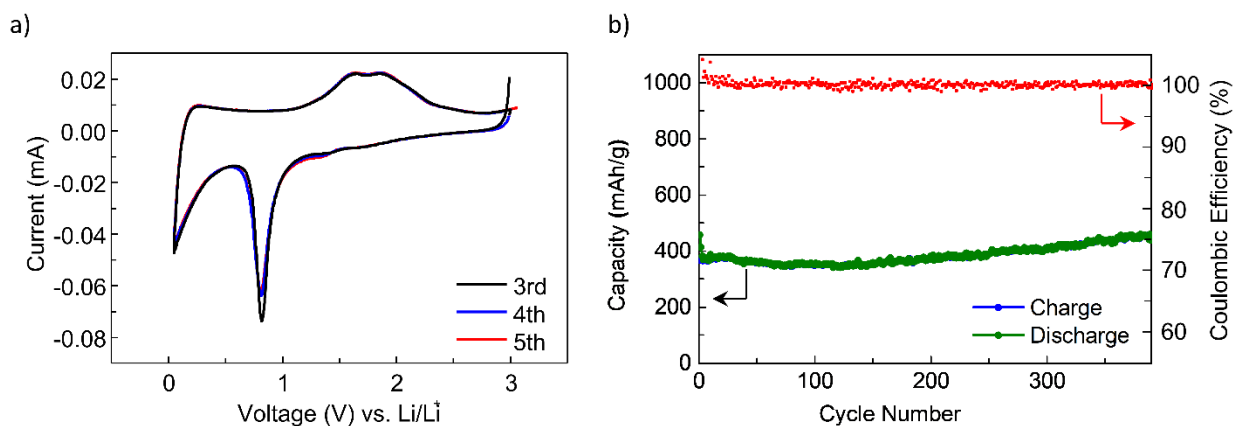


Figure S3: (a) cyclic voltammetry and (b) long-term cycling at 2.7 C

Notes and references

1. Wang B, Chen JS, Wu H Bin, Wang Z, Lou XW. Quasiemulsion-templated formation of $\alpha\text{-Fe}_2\text{O}_3$ hollow spheres with enhanced lithium storage properties. *J Am Chem Soc.* 2011;133:17146–8.